Cell Reports, Volume *38*

Supplemental information

Intestinal Gpr17 deficiency improves glucose metabolism by promoting GLP-1 secretion

Shijun Yan, Jason M. Conley, Austin M. Reilly, Natalie D. Stull, Surabhi D. Abhyankar, Aaron C. Ericsson, Tatsuyoshi Kono, Andrei I. Molosh, Chandrashekhar A. Kubal, Carmella Evans-Molina, and Hongxia Ren

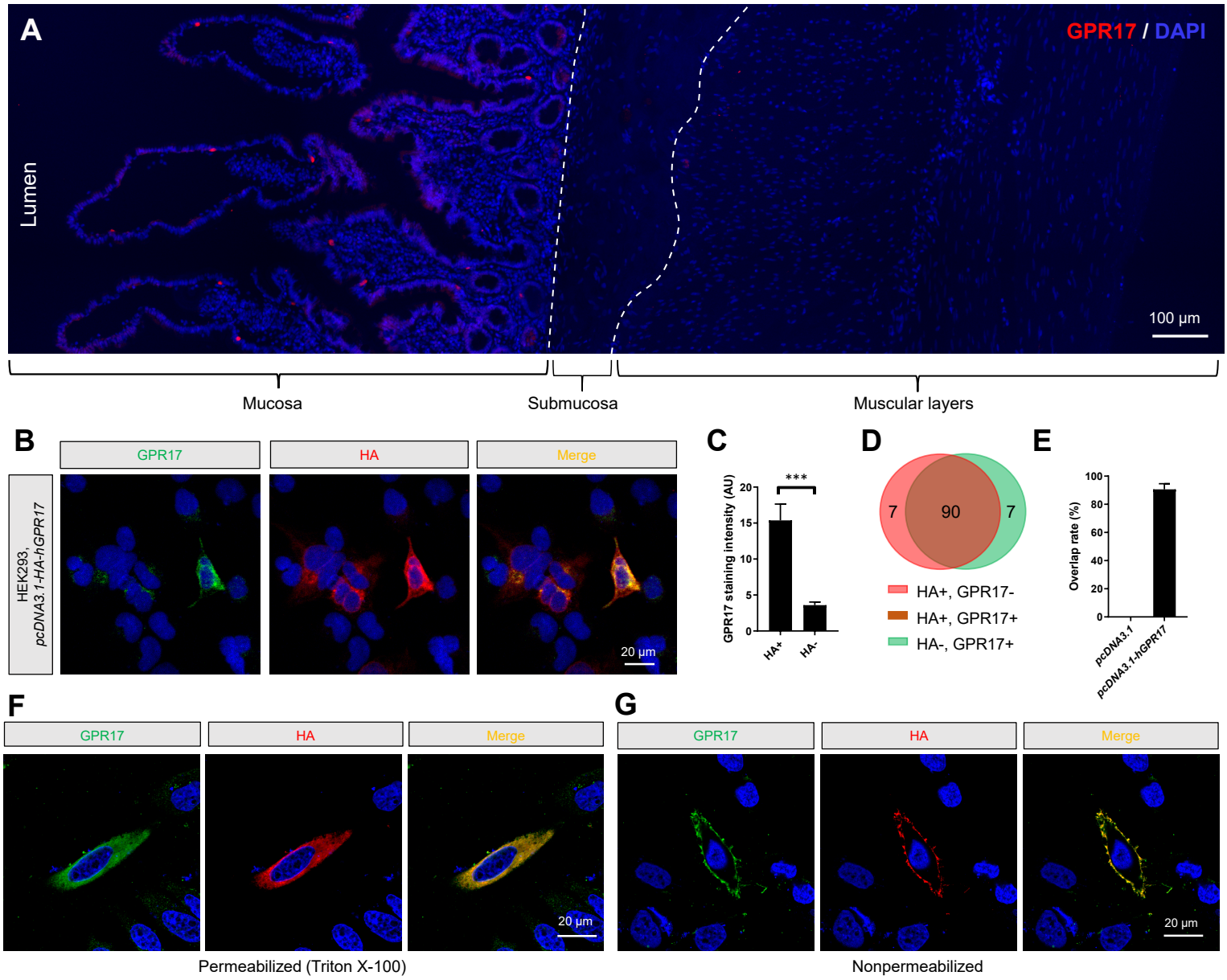

Supplemental Figure S1. Validation of GPR17 antibody specificity and tissue distribution of Gpr17 in mice. Related to Figure 1. A. Immunohistochemistry staining of GPR17 in human small intestine. GPR17 was detected in mucosal epithelium layer but not in submucosa or muscular layers. **B.** Co-immunostaining of GPR17 and HA in HEK293 cells transiently transfected with pcDNA3.1-HA-hGPR17. **C.** Gpr17 staining intensity in HA+ and HA- cells (n=10 image fields). **D.** Venn diagram depicting the counts of single-stained or double-stained cells. **E.** Overlap rate showing percentage of double-stained cells in all HA+ cells (n=10 image fields). **F-G.** Representative images of total (**F**) or cell-surface (**G**) staining of GPR17 and HA in HeLa cells transiently transfected with pcDNA3-HA-hGPR17. Cells were permeabilized by 0.1% Triton X-100 for total GPR17 staining or nonpermeabilized for cell-surface GPR17 staining. Unpaired two-tailed Student's t-test, ***p<0.001. Data are displayed as means ±SEM.

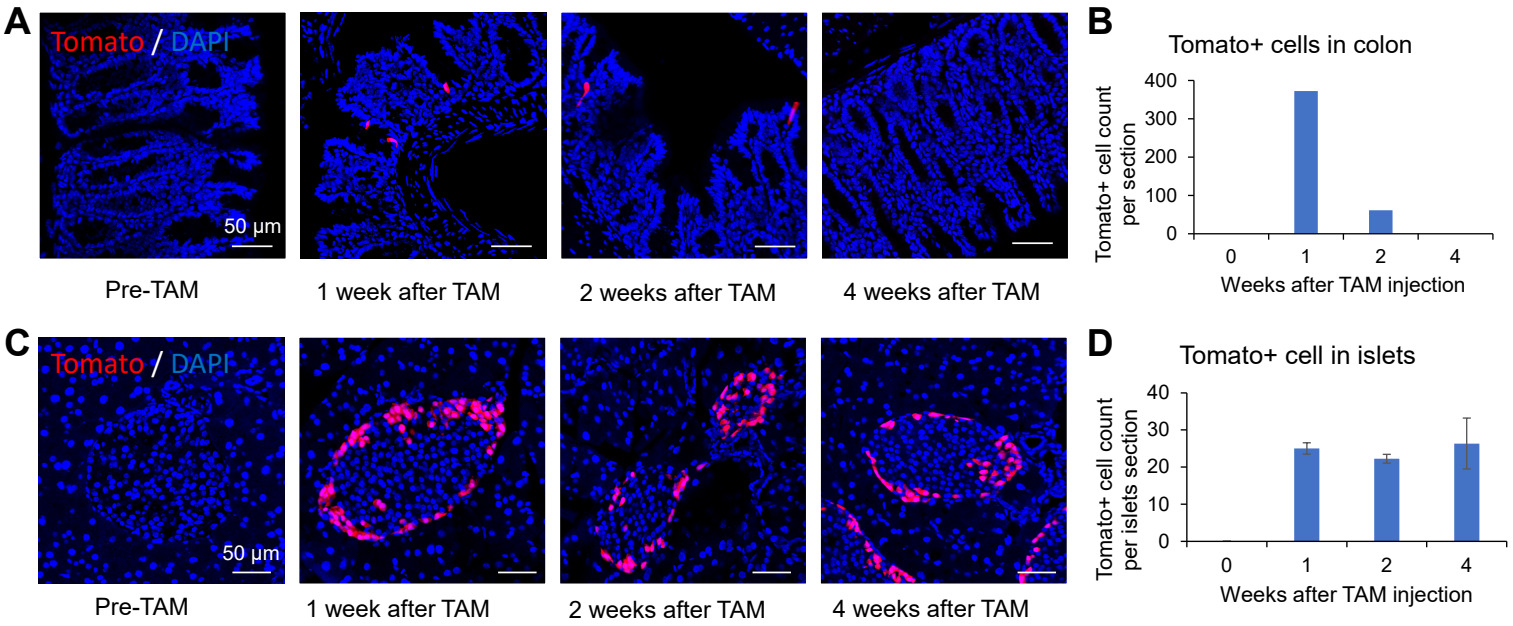

Supplemental Figure S2. Cre recombinase was activated by tamoxifen in both islets and gut of *Rosa-tdTomato;Gcg-CreERT* mice. Related to Figure 3. A-B. *Gcg* expressing cells in gut were labeled by red fluorescence (tdTomato) after tamoxifen-induced Cre recombinase activation. The hit targeting gut was temporary due to the fast-refreshing rate of gut epithelium. Cells were counted in "swiss roll" sections of the whole colon (n=1 mouse). C-D. *Gcg* expressing cells of islets were labeled by red fluorescence (tdTomato) after tamoxifen-induced Cre recombinase activation. The hit targeting islets was sustained during the observance period. Cells were counted in 3~4 islets per mouse (n=1 mouse).

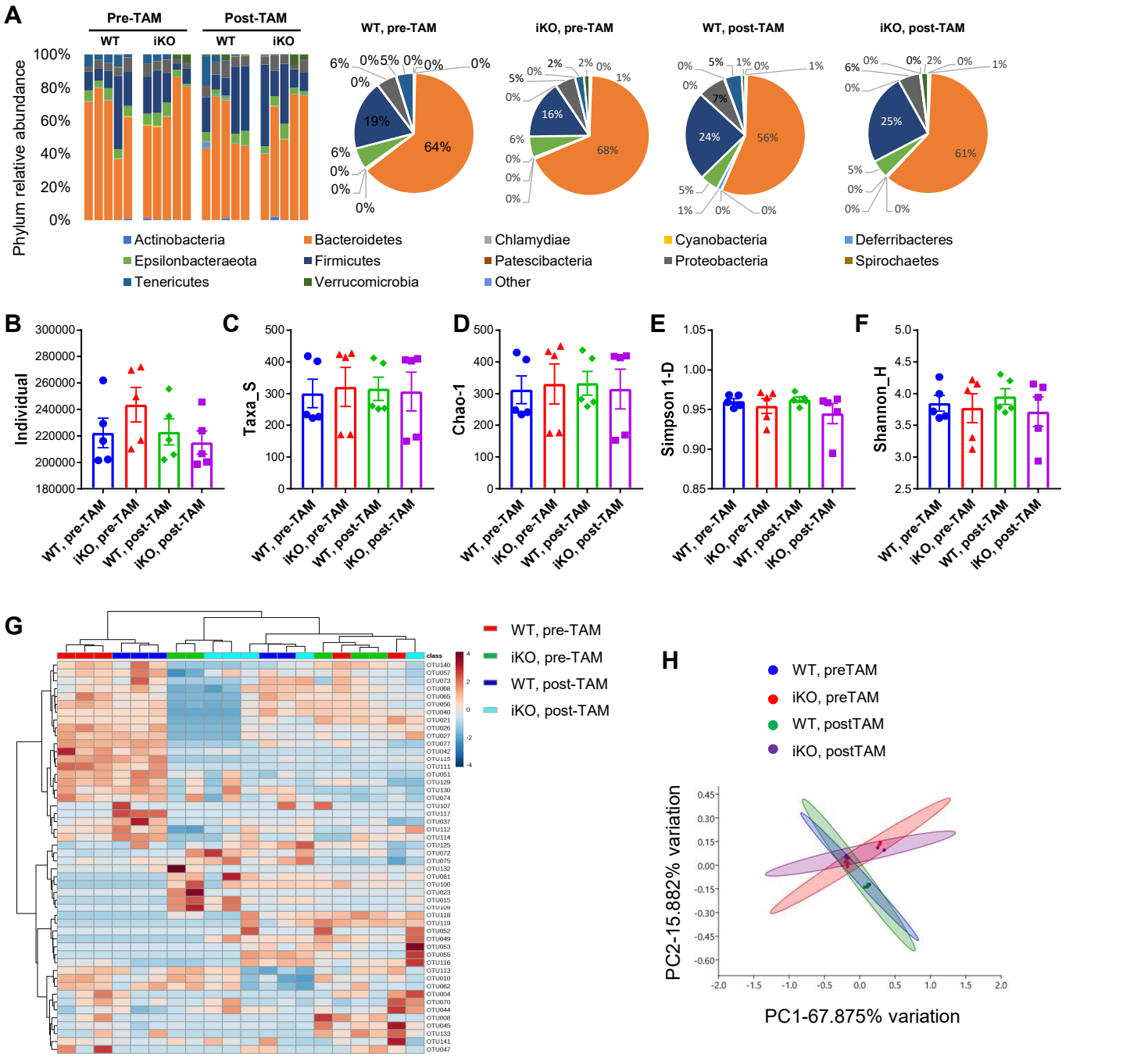

Supplemental Figure S3. Microbiota analysis of inducible intestinal Gpr17 KO mice before and after tamoxifen injection. Related to Figure 5. A. Stacked bar chart and pie chart showing the relative abundance of phyla in feces of chow-fed WT and iKO mice before and after tamoxifen injection (n=5 mice for each group). **B-F.** Sample richness (b, individual; c, Taxa_S, detected richness; d, Chao-1, predicted richness) and alpha-diversity (e, Simpson 1-D; f, Shannon H) were not significantly changed. **G.** Heatmap showing the relationship of fecal samples from WT and iKO mice before and after tamoxifen injection. Top-50 differentially abundant OTUs (rows) and samples (columns) were arranged. **H.** Principal component analysis (PCA) of microbiota. Unpaired two-tailed Student's t-test were performed. Data are displayed as means ±SEM.

Table S1. List of primers and oligonucleotides. Related to STAR methods.

Primer for RT-qPCR	Oligo Sequence
Human *GPR17*-F	GCCATAGTGCTGGCCATCTT
Human *GPR17*-R	TACATGATGGGGTCGAGTGC
Mouse *Gpr17*-F	GGAGCACCATCTAGAGCACCCT
Mouse *Gpr17*-R	GGCTGCCTCCAGACCGTTCAT
Mouse *Gcg*-F	GGCACATTCACCAGCGACTA
Mouse *Gcg*-R	GTCCCTTCAGCATGCCTCTC
Mouse *Gip*-F	AACTGTTGGCTAGGGGACAC
Mouse *Gip*-R	GAAAGTCCCCTCTGCGTACC
Mouse *Pyy*-F	CCTGCTCATCTTGCTTCGGA
Mouse *Pyy*-R	ACTGGTCCAAACCTTCTGGC
Human *RPLP0*-F	GGCAGCATCTACAACCCTGA
Human *RPLP0*-R	CACAGACAAGGCCAGGACTC
Mouse *β-actin*-F	CAGCTTCTTTGCAGCTCCTT
Mouse *β-actin*-R	CACGATGGAGGGGAATACAG